Journal of Cleaner Production 265 (2020) 121440

Contents lists available at ScienceDirect

Journal of Cleaner Production

journal homepage: www.elsevier.com/locate/jclepro

A clean approach of biodiesel production from waste cooking oil by using single phase $BaSnO_3$ as solid base catalyst: Mechanism, kinetics & E-study

Tania Roy [a], Shalini Sahani [a], Devarapaga Madhu [b], Yogesh Chandra Sharma [a, *]

[a] Department of Chemistry, Indian Institute of Technology (BHU) Varanasi, Varanasi, 221005, India
[b] Center for Lipid Science & Technology, Indian Institute of Chemical Technology, Hyderabad, 500007, India

ARTICLE INFO

Article history:
Received 4 January 2020
Received in revised form
2 March 2020
Accepted 29 March 2020
Available online 10 April 2020

Handling Editor: Maria Teresa Moreira

Keywords:
Barium stannate
Waste cooking oil
Optimization
E-R mechanism
Kinetic study
E-factor

ABSTRACT

The current policies of govt. of India on biodiesel production and commercialization have encouraged to explore this area widely. In this study barium stannate perovskite was synthesized to evaluate its activity and stability as a solid base catalyst in biodiesel synthesis from waste cooking oil (WCO). Physicochemical characterizations of the catalyst and feedstock were thoroughly investigated by various techniques. Experimental planning was executed to investigate the impact of various parameters on methyl esterification reaction. 98% fatty acid methyl ester (FAME) conversion was achieved at following optimum reaction condition: Ba: Sn atomic ratio 1:1, catalyst activation temperature 850 °C, oil to methanol molar ratio 1 : 16, catalyst concentration 2.5 wt%, temperature 65°C, time 25 min. Catalyst endurance test suggested that the $BaSnO_3$ has the appreciable catalyzing potency and stability for several times use. The characteristic difference in FTIR of fresh catalyst and used catalyst indicated the mode of interaction between catalyst and reactants. On this basis a plausible E-R mechanism has been proposed. Kinetic study of the transesterification process by using $BaSnO_3$ revealed that this process was base catalyzed transesterification and followed non spontaneous endothermic pathway. High turnover frequency and low E-factor of the catalyst implied that biodiesel production from waste cooking oil by using $BaSnO_3$ was fast, efficient and benign to all environmental prospective.

1. Introduction

The growing population, urbanization and industrialization have led to tremendous enhancement in energy consumption by 2.3% per year (Omer, 2008). The transportation sector itself consumes 30% of the world's total energy consumption (Conti et al., 2016). The limited non renewable resources are steeply depleted and going to be worn out very soon. Moreover, burning of fossil fuel induces toxic emissions to the environment; which should further cause of a number of environmental problems (Hardy, 2003). Thus, researchers through all over the world are attending their focus to encounter the aforementioned challenges, and ensure the future energy security. As first generation biofuel, biodiesel globally attracts more attention as an alternative of petrodiesel (Knothe, 2010). Using biodiesel has number of advantages like biodegradability, technical feasibility, lower greenhouse gas (GHG) emissions, non-toxicity, and carbon neutrality (Bozbas, 2008).

Nowadays, used cooking oil has been admired as potential feedstock for a continuous resource of biodiesel production (Su et al., 2013). According to Food Safety and Standards Authority of India's (FSSAI) report, it is claimed that India is the world's biggest consumer of cooking oil (vegetable oil) and consumes 225 lack tones per year, of which 30% get discarded as waste cooking oil. This large amount of oil neither be introduced in food chain due to high acid value nor disposed off as it surely reciprocates several environment problems. Furthermore, biodiesel synthesis from waste cooking oil encourages the concept of 'waste to well' and deliberates a smart waste management. FSSAI also claimed that India has the potential to recover 220 Cr liters of WCO to produce biodiesel by the year 2022 through coordinated action. Thus waste cooking oil has the well potency to become a sustainable resource for industry level biodiesel production in India. Raw material accounts about 60–70% of the final cost of biodiesel synthesis which can also be deduced by using waste cooking oil. Additional cost of

* Corresponding author.
E-mail address: ysharma.apc@itbhu.ac.in (Y. Chandra Sharma).

https://doi.org/10.1016/j.jclepro.2020.121440
0959-6526/

biodiesel processing can be reduced by using an efficient heterogeneous catalyst, and recovering the byproduct (glycerol) of the transesterification reaction for further commercialization to its value aided product (Mohadesi et al., 2014).

Homogeneous catalysts are associated with a number of demerits such as non recyclability, high corrosive nature to the equipments, toxic and hazardous chemical characteristics. It also demand additional purification step and produce large amount of waste water (solvent). Comparatively, heterogeneous catalyst is more susceptible for economic production as it can easily be removed and reused for multiple times with appreciable efficacy. Alkali and alkaline earth metal oxides are very promising for heterogeneous base catalyzed transesterification of oil. Singh and Fernando (2007) has reported that BaO as a heterogeneous catalyst is efficient to derive biodiesel from soybean oil at high temperature of 215 °C. Yan et al. (2007) accomplished that BaO possessed the best catalytic activity compared to MgO, CaO, and SrO due to its highest alkalinity. Similar result was also observed by Patil and Deng (2009). Balakrishnan et al. (2013) reported that barium supported on waste marble as heterogeneous base catalyst produced 88% FAME yield at moderated reaction condition. Basically, barium enhanced the catalytic efficiency of waste marble. A very interesting study on biodiesel production was reported by Martinez-Guerra and Gude (2014). They carried out the transesterification reaction using barium oxide catalyst under simultaneous microwave and ultrasound irradiation and it was found that within 2 min the reaction was completed and showed around 95% yield. An impactful coordination of an active species and a stable support always contribute to impressive efficacy and long durability of the catalyst. SiO_2 (Mierczynski et al., 2015), Al_2O_3 (Mohadesi et al., 2014), CuO (Yang et al., 2010) etc are reported as support materials of BaO for transesterification process. Many researchers have ascertained that SnO_2 has the nice properties for being a stable support in heterogeneous catalyst. Likewise, tin supported catalyst SnO_2–SiO_2 showed impressive effectiveness towards transesterification of soybean oil and in this Sn–O bond itself acts as Lewis acid site or the active site for the catalysis (Xie et al., 2011). Based on the nature of the active component, both acidic and basic tin oxide supported heterogeneous catalyst has been designed for methyl esterification reaction. As for example, an excellent tin based acid catalyst SO_4^{2-}/SnO_2–SiO_2 was synthesized for transesterification of high free fatty acid content low grade oil (Lam et al., 2009), whereas a basic catalyst CaO–SnO_2 (Ca: Sn = 4:1) was prepared to produce biodiesel from soybean oil with 83.9% FAME conversion (Xie and Zhao, 2013). It can be understood that waste cooking oil is a potential feedstock and that BaO with SnO_2 support has emerged as a suitable catalyst for base catalyzed transesterification reaction.

In this study, the major objectives were to synthesis an efficient barium stannate catalyst for transesterification of WCO and develop a biodiesel production route which must be cost effective and clean or green with respect to environmental parameters. Many researchers have suggested that reuse of industrial wastes like red mud, metakaolin, etc. or manufacture of ecofriendly materials like geopolymers from industrial wastes are cleaner approach with respect to solid waste management (Nenadović et al., 2017; Mucsi, 2017; Bošković et al., 2019; Kljajević et al., 2019; Mladenović et al., 2020). Likewise, using waste cooking oil as feedstock material for biodiesel production would be welcomed as eco-friendly way out of open disposal of liquid waste. Moreover, the cleanness of the process or in other words extent of harmful effect of waste generation on environment during the process should be explored with serious concern. In our study the cleanness of the biodiesel production from WCO using barium stannate catalyst was judged w. r. t. environmental parameters as environmental factor (E-factor) and process mass index (PMI).

2. Materials and methodologies

2.1. Feedstock and chemicals used

WCO was selected as potential feedstock for biodiesel synthesis and it was collected from cafeteria of Indian Institute of Technology-Banaras Hindu University, Varanasi. Preliminary, the collected oil was filtered to separate the solid particles and then dried to eliminate water. Before using it in transesterification, some important physico-chemical properties were investigated as shown in Table 1. The chemicals as Tin (IV) chloride pentahydrate ($SnCl_4.5H_2O$ 98%, Sigma Aldrich) and barium nitrate ($Ba(NO_3)_2$, ACS reagent $\geq$ 99.9%, Sigma Aldrich) was used as precursor material and was purchased from Advance Scientific (Varanasi, India). Ammonium hydroxide (NH_4OH, ACS reagent 28–30% NH_3, Merck), methanol (MeOH, EMSURE grade 99.9%, Merck) and other chemicals as well as reagents were used directly without purification or distillation.

2.2. Catalyst preparation via wet impregnation method

The catalyst barium stannate was prepared by wet impregnation of tin hydroxide into barium nitrate solution. At first, barium hydroxide was prepared by precipitation method. The required amount of tin (IV) chloride pentahydrate ($SnCl_4.5H_2O$) was dissolved in 50 ml deionized water (DI). Then 25% ammonia solution was added dropwise to the tin chloride solution under constant stirring up to the pH value 9. After ensuring the complete precipitation of tin hydroxide, the white slurry mixture was left under constant agitation for 1 day. The day after, precipitate was isolated from the mother liquor by vacuum filtration and washed several times by DI water to remove the chloride ion and other impurity ions. Then fresh $Sn(OH)_4$ precipitate was dried overnight in hot air oven followed by crushing into fine particle of $Sn(OH)_4$. Pure tin oxide (SnO_2) was prepared by calcine tin hydroxide at 850 °C for 5h in air muffle furnace.

The solid barium stannate catalyst with different Ba/Sn atomic ratios (1 : 1, 2 : 1, 1 : 2) were prepared by impregnating $Sn(OH)_4$ powder into a saturated barium nitrate solution. In typical catalyst preparation of $BaSnO_3$, 1 g of $Sn(OH)_4$ powder was impregnated into the aqueous solution of 1.21g $Ba(NO_3)_2$. The mixture was agitated at 80 °C to get its slurry form. Then it was dried at 110 °C for overnight in air oven. The obtained solid product was finely crushed and calcined at 850 °C in an air muffle furnace for 5h (Xie and Zhao, 2013).

The synthesized barium stannate samples having different Ba: Sn atomic ratios, designated as BSO (Ba: Sn 1 : 1), 2BSO (Ba: Sn 2 : 1), and B2SO (Ba: Sn 1 : 2), were characterized by various techniques as mentioned below.

2.3. Characterizations

The thermal gravimetric analysis (TGA) of uncalcined barium stannate was performed on EXSTAR TG/DTA 6300 instrument of Central Instrumental Facility Center, IIT Roorkee. The TGA analyzer was run between the heating ranges of 35 °C–1300 °C with a heating rate of 10 °C/min in inert atmosphere (N_2). Powder X-ray diffraction (XRD) of catalyst samples was registered on Rigaku MiniFlex-300/600 with a potential external gradient of 40 kV and 15 mA anode current. The diffractogram was scaled at a 2θ range of 10° to 80° at 10°/min scan rate along with step width of 0.02° (2θ) and the resultant data was verified by Joint Committee on Powder Diffraction Standards (JCPDS) to evaluate the synthesized phase of

Table 1
Physico-chemical properties of feedstock (WCO).

Properties	Waste cooking oil	ASTM standard method
Color	Gardner 2 max	D 1544
Acid value (mg KOH/g oil)	1.53	D 664
Saponification number (mg KOH/g oli)	204.6	D 9407
Iodine number (mg I_2/g)	133.8	D 2500
Calorific value (MJ/Kg)	38.44	D 240
Viscosity (mm^2/s) at 40 °C	68.21	D 7110
Density (Kg/m^3) at 27 °C	906.2	D 4052
Refractive Index	1.46	D 1717
pH	5.8	–

the catalyst. Attenuated total reflection-Fourier transformed Infrared spectra (ATR-FTIR) of catalyst samples were executed on ALPHA BRUKER Eco and ZnSe crystal was used as source of evanescent wave. All FTIR spectra were recorded with 24 scanning rate and 4 cm^{-1} resolution within infrared range of 400–4000 cm^{-1}. X-ray photoelectron spectrometer (XPS) analysis was carried out on K-Alpha X-ray Photoelectron Spectrometer (XPS) System of Thermo-Fisher Scientific. Monochromated and micro-focused Al K_α was used as X-ray source in XPS analyzer. The binding energy of C 1s i.e. 284.8 eV was considered as the reference to calibrate the binding energies of the corresponding elements present in the catalyst. Surface morphology of the synthesized catalysts was visualized by NOVA Nano SEM 450, a scanning electron microscope (SEM) which was associated with EDAX-Ametek detector for quantitative elemental detection by energy dispersive X-ray spectroscopy. The surface characterization of the catalyst samples were executed by nitrogen adsorption-desorption isotherm method on Micromeritics ASAP 2020V1.05 software, a BET surface area analyzer. Basicity (i.e. the number of basic sites present per gram of catalyst sample) of pure SnO_2 and barium stannate samples were measured by Hammett indicator-titration method (Hashimoto et al., 1986). For this purpose a series of Hammett indicators: neutral red ($H_- = 6.8$), bromothymol blue ($H_- = 7.2$), phenolphthalein ($H_- = 9.3$), tropaeolin-O ($H_- = 11.1$), and 2,4-dinitroaniline ($H_- = 15.0$) were used. In this case, firstly, 25 mg of catalyst sample was dispersed in 5 ml methanol. Then 2 to 3 drops of indicator solution was added to it. The catalyst solution became adopt a specified colour according to pK_a range of the aforementioned indicators. After 30 min shaking, the catalyst-indicator solution was left for 15 min to reach the equilibrium. Finally, it was titrated against the 0.01 M benzoic acid. The titer value indicated the number of basic sites present per gram of catalyst (mmol/g).

Compositional percentage of fatty acids present in feedstock was quantified by Agilent 6890N gas chromatograph which is constituted by a column Agilent Db-225 capillary (30 m length × 25 mm inner diameter × 0.25 μm film thickness) and a flame ionisation detector (FID). Supelco 37 Component FAME Mix (CRM 47885) helped in comparing the retention time for confirming the constituent fatty acids of feedstock. ^1H NMR and ^{13}C NMR of WCO and the derived biodiesel were performed on BRUKER 500 Ascend™ 500 (advance III HD) instrument by using d-chloroform and trimethylsilane as a solvent and internal standard respectively.

2.4. Transesterification and product analysis

Before use in transesterification, some prior refining treatments of the feedstock were necessary to carry out. First, the suspended solid impurities were separated by filtration method and second, the oil was heated overnight in air oven to evaporate the moisture content into the feedstock. Then acid value of the refined feedstock was evaluated by following procedure described in ASTM D664, and it was found within permissible limit i.e. <3 mg KOH/g for direct use of feedstock in transesterification reaction. The catalytic efficacy of barium stannate ($BaSnO_3$) as solid base catalyst in biodiesel production was examined by lab scale transesterification reaction. Such transesterification reaction was conducted in 250 ml three-neck R.B (round bottom) flask which was assembled with a condenser, a mechanical stirrer, and a thermometer. The above arrangement was fitted into a temperature controlled oil bath. Primarily, the catalyst was activated by eliminating surface moisture in air oven for 30 min at 110 °C before putting it into the transesterification reaction. Then, required gram of activated catalyst was dispersed into required amount of methanol at room temperature for 15 min followed by addition of 10 ml feedstock. Temperature of the water bath was then increased to the desire reaction temperature. After getting the desire reaction temperature, the reaction mixture was refluxed under constant stirring for 25 min (the optimum reaction duration). The product mixture was first filtered to separate out the catalyst and washed thoroughly and subsequenty by methanol and ethanol. Used catalyst was dried, reactivated and reused; whereas, the filtrate was poured into a separating funnel and hold it for one day. The day after the whole mixture was separated in three distinct phases of glycerol (bottom), FAME or biodiesel (middle) and excess methanol (top). These were collected in three distinct jars. Glycerol as the byproduct of FAME was used in further value added product synthesis; whereas, the excess methanol was distilled and further used in several lab work. The FAME Conversion and yield were estimated by following equations (1) and (2) in ^1HNMR spectroscopy of synthesized biodiesel (Birla et al., 2012):

$$\%\ \text{of FAME Conversion} = (2A_{ME})\ (3A_{\alpha\text{-}CH2}) \times 100 \quad (1)$$

$$\%\ \text{of FAME Yield} = (A_{ME})\ (A_{\alpha\text{-}CH2}) \times 100 \quad (2)$$

A_{ME} and $A_{\alpha\text{-}CH2}$ are designated as integration of methyl ester ($-OCH_3$) protons and alpha-methylene (CH_2-CO-) protons respectively.

Several optimizations such as Ba: Sn atomic ratio, calcination temperature of catalyst, oil to methanol molar ratio (varied from 1:4 to 1:24), reaction temperature(varied from 35 to 75 °C), catalyst weight % (varied from 0.5 wt% to 3 wt%), and time (varied from 5 to 30 min) were performed by following the aforementioned procedure of transesterification reaction. For a single datum, the particular experiment was reciprocated at least three times and the average of three outcomes was granted as final data.

2.5. Kinetic and thermodynamic study

Basically kinetic study relates the rate of the reaction to reaction

temperature for a particular process. The kinetics information as rate constant, activation energy and frequency factor regarding methyl esterification of WCO using BSO as heterogeneous catalyst was investigated by constructing a kinetic model on the basis of previous studies.

The methyl esterification of a triglyceride molecule proceeds in three consecutive reversible reactions as shown below:

$$TGL + MeOH \leftrightarrow FAME + DGL \quad (3a)$$

$$DGL + MeOH \leftrightarrow FAME + MGL \quad (3b)$$

$$MGL + MeOH \leftrightarrow FAME + GLY \quad (3c)$$

The overall stoichiometric equation is written as:

$$TGL + 3MeOH \leftrightarrow GLY + 3FAME \quad (4)$$

Where, TGL is triglyceride, DGL is diglyceride, FAME is fatty acid methyl ester (biodiesel), GLY is glycerol.

It is clear from above equation (4) that the rate depends on both concentrations of triglyceride and methanol. As all the three steps of the transesterification process are reversible, so stoichiometrically excess amount of methanol would divert the reaction equilibrium more towards the product side. The concentration of methanol almost would be unaffected during the reaction due to its presence in extensive amount, and the rate of the reaction depends only on the concentration of triglyceride. So, considering the aforementioned fact, it is mentioned that a first order kinetics is more logical for such reaction and the rate equation can be written as:

$$-d[TGL]/dt = k[TGL] \quad (5)$$

k is the rate constant at a particular temperature.

From mass balance,

$$X_{FAME} = 1 - ([TGL]_t/[TGL]_0) \quad (6)$$

$$So, [TGL]_t = [TGL]_0 \times (1 - X_{FAME}) \quad (7)$$

X_{FAME} refers the methyl ester conversion. Integrating the equation (7) we get the following equation in terms of X_{FAME}:

$$-\ln(1 - X_{FAME}) = k \times t \quad (8)$$

Rate constant of the reaction can be find out from the slope of $-\ln(1- X_{FAME})$ versus time t (min) plot (Encinar et al., 2018). Activation energy or threshold energy of the reaction was estimated by the help of Arrhenius plot. Considering Arrhenius equation (Chen et al., 2020), the rate constant (min^{-1}) is related to activation energy (E_a in $kJ.mol^{-1}$) and reaction temperature (T in Kelvin) as:

$$k = A \exp(-Ea/RT) \quad (9)$$

Simplifying the equation (9) we get:

$$\ln k = \ln A - Ea/RT \quad (10)$$

Where the A is the Arrhenius constant or frequency factor in min^{-1} and R is the gas constant (8.314×10^{-3} $kJ.K^{-1}.mol^{-1}$). The slope and intercept of the plot of ln k versus 1/T help to derive reaction activation energy and frequency factor respectively.

According to the fundamental thermodynamic equation regarding Gibb's free energy is

$$\Delta G = \Delta H - T\Delta S \quad (11)$$

Where, ΔG, ΔH, and T are Gibb's free energy, enthalpy of reaction and absolute temperature of reaction respectively.

Subordinately, Gibb's free energy of activation ($\Delta G^{\#}$) can be derived from Eyring – Polanyi equation (Galvan et al., 2013) which leads to

$$k = k_b T/h \times \exp(-\Delta G^{\#}/RT) \quad (12)$$

Now, substituting the $\Delta G^{\#}$ term by $\Delta H^{\#}$ and $\Delta S^{\#}$ in equation (12) we get,

$$k = k_b T/h \times \exp[(-\Delta H^{\#} + T\Delta S^{\#})/RT \quad (13)$$

or,

$$\ln(k/T) = [\ln(k_b/h) + (\Delta S^{\#}/R)] - (\Delta H^{\#}/RT) \quad (14)$$

. Where, $\Delta H^{\#}$ and $\Delta S^{\#}$ are enthalpy of activation and entropy of activation, h is Planck constant (6.626×10^{-34} J s), k_b is Boltzmann constant (1.38×10^{-38} $J.K^{-1}$). Slope and intercept of the linear regression plot of ln(k/T) Vs 1/T refer the value of $\Delta H^{\#}$ and $\Delta S^{\#}$. Gibb's free energy of activation was evaluated from the equation (11).

3. Results and discussion

3.1. Catalyst characterization

Physical characterizations as TGA-DTA, FTIR, XRD, SEM-EDX analysis, BET surface area analysis and basicity analysis of the catalyst barium stannate samples (BSO, 2BSO, B2SO) along with pure tin oxide (SnO_2) were carried out to interpret their the chemical behavior in transesterification reaction.

3.1.1. Thermo-gravimetric analysis (TGA) with differential thermal analysis (DTA)

The thermal disintegration profile of the uncalcined barium stannate (Ba: Sn = 1 : 1) sample has been shown in Fig. 1. It was observed that during the heat treatment process (35–1000 °C), total ~ 40% mass loss was occurred in two events. Initial mass loss

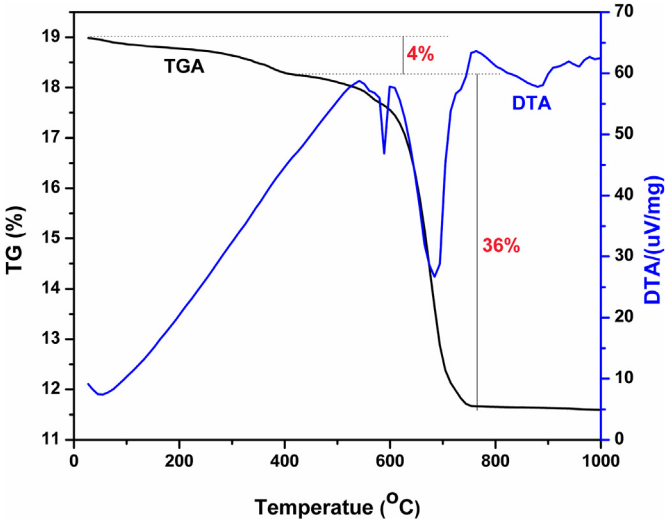

Fig. 1. TGA-DTA plot of catalyst $BaSnO_3$.

of 4% appeared up to 400 °C due to elimination of physisorbed surface water and the crystalline water. Next, 36% mass loss was taken place between 400 °C to 758 °C. Regarding this second mass loss event two corresponding endothermic DTA peak around 590 °C and 685 °C were found. This has anticipated that this major mass loss is associated with $BaSnO_3$ formation from their respective precursor moiety by decomposition of nitrates and hydroxides. Substantially, the corresponding DTA peaks were attributed due to thermal decomposition of barium nitrate and tin hydroxide respectively (Roy et al., 2018). After 758 °C, no mass loss was found up to 1000 °C in TGA profile. This means the catalyst became thermally stable at a calcination temperature of 758 °C and the optimum activation temperature of barium stannate should be greater than 758 °C.

3.1.2. X-ray powder diffraction (XRD) analysis

The prepared catalyst samples (BSO, 2BSO, B2SO) were characterized by powder XRD to figure out the phases formed into the material. The relative diffractogram in Fig. 2A has implied that the different phases were formed in catalyst samples having different Ba/Sn atomic ratio. The XRD pattern of SnO_2 powder having no sharp peak indicates the complete amorphous state of tin oxide. The major XRD peaks of the barium stannate compound (BSO, 2BSO, B2SO) positioned at 2θ (hkl) = 30.7° (110), 37.9° (111), 44° (200), 54.6° (211), 64° (220), 72.7° (013), 81° (222), 89° (123) were assigned as characteristic peaks of primitive cubic lattice of $BaSnO_3$, confirmed by JCPDS file no. 74–1300 (Wu et al., 2012). BSO was existed in a pure phase of $BaSnO_3$. However, 2BSO (Ba/Sn 2:1) and B2SO (Ba/Sn 1:2) had $BaSnO_3$ along with additional phase of stoichiometrically excess component. Ba was present in excess amount in 2BSO and Sn was excess in B2SO. Such excess Ba of 2BSO sustained as $BaCO_3$ phase (# JCPDS file no. 712394), whereas excess Sn of B2SO was in form of SnO_2 (# JCPDS file no. 880287).

A scrutiny on catalyst activation temperature or the calcination temperature and calcination time were performed to investigate the impact of high temperature and its duration in different phase formation and their stability. Fig. 2B has manifested that BSO got the pure $BaSnO_3$ phase at the calcination temperature of 550 °C but the phase became more prompt at 850 °C. This result substantiates the TGA result which primarily sketches an idea about the activation temperature which might be greater than 758 °C. It is also found that the catalytic phase i.e. $BaSnO_3$ of BSO was completely activated at 850 °C for 5 h as shown in Fig. 2C.

3.1.3. Attenuated total reflectance – fourier transform infrared (ATR-FTIR) analysis

A comparative ATR-FTIR study of barium stannate catalyst samples was inspected to support the facts deliberated in XRD analysis. The functional groups present in tin hydroxide and catalyst samples (BSO, 2BSO, B2SO) were analyzed and compared as shown in Fig. 3. FTIR of tin hydroxide (Fig. 3a) shows intense broad peak at 3700 cm^{-1} to 3400 cm^{-1} and sharp peak at 1637 cm^{-1} which represent the presence of hydroxyl group in $Sn(OH)_4$. Another broad peak at 3290 cm^{-1} to 2480 cm^{-1} along with a sharp peak at 1404 cm^{-1} indicate that some of NH_4OH might be trapped into the $Sn(OH)_4$ during synthesis. The characteristic Sn–O and Sn–OH peaks were observed at 663 cm^{-1} and 554 cm^{-1} respectively (Xie and Zhao, 2013). Fig. 3d has revealed that the catalyst BSO having Ba/Sn atomic ratio 1 : 1 has the highest intensity Sn–O–Sn stretching frequency at 620 cm^{-1} which implies that BSO existed in pure $BaSnO_3$ perovskite form (Sakthiraj et al., 2018). Due to the moisture affinity of barium, a mild stretching frequency of surface moisture has also been observed at 3418 cm^{-1}. FTIR of 2BSO (Ba/Sn 2 : 1) has displayed the characteristic carbonate peaks at 1438 cm^{-1} (asymmetric stretching of C–O), 1058 cm^{-1} (symmetric stretching of C–O), 876 (in-plane bending in of O–C–O) along with Sn–O–Sn stretching frequency of $BaSnO_3$ phase and broad –OH of water contamination, as shown in Fig. 3c (Deepa et al., 2011). Barium has immense affinity towards carbon dioxide and moisture which reflects as result in FTIR spectra of 2BSO (Kwon et al., 2015).

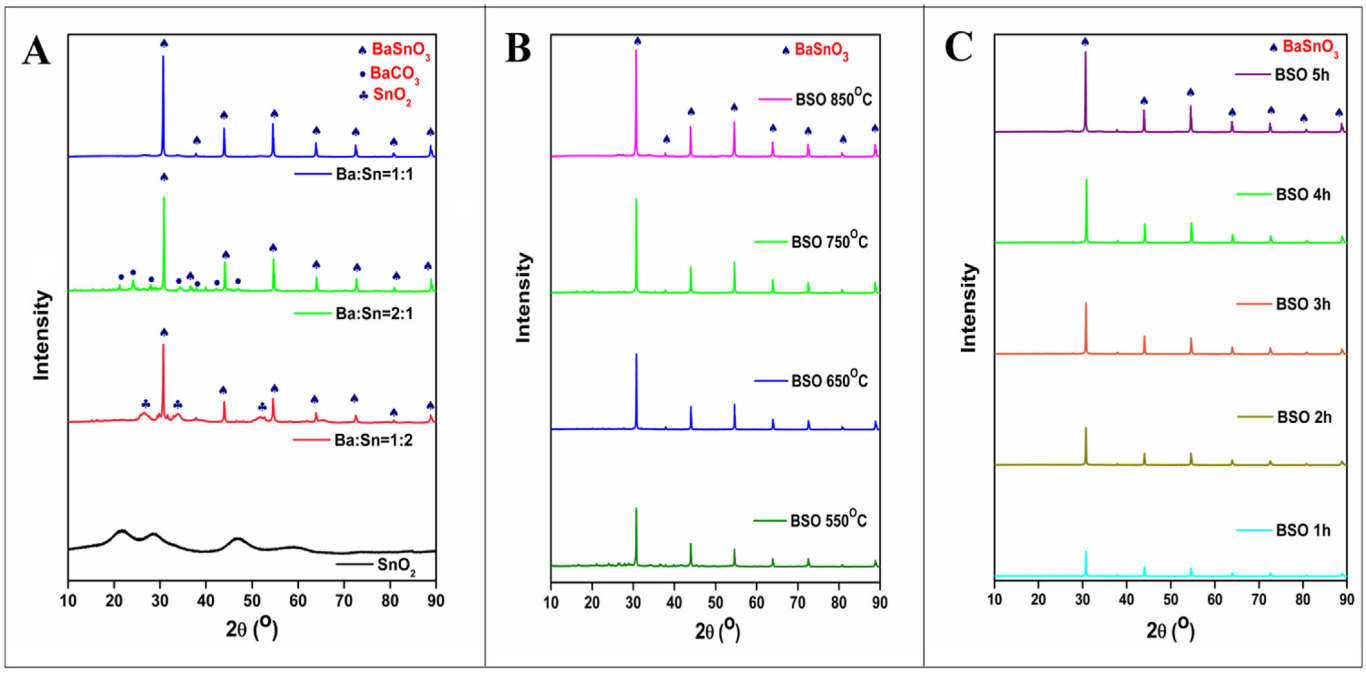

Fig. 2. Comparative A) XRD of barium stannate compounds having different stoichiometric ratio of Ba:Sn, B) XRD of $BaSnO_3$ compound calcined at different temperature C) XRD of $BaSnO_3$ compound calcined at 850 °C for different calcination time.

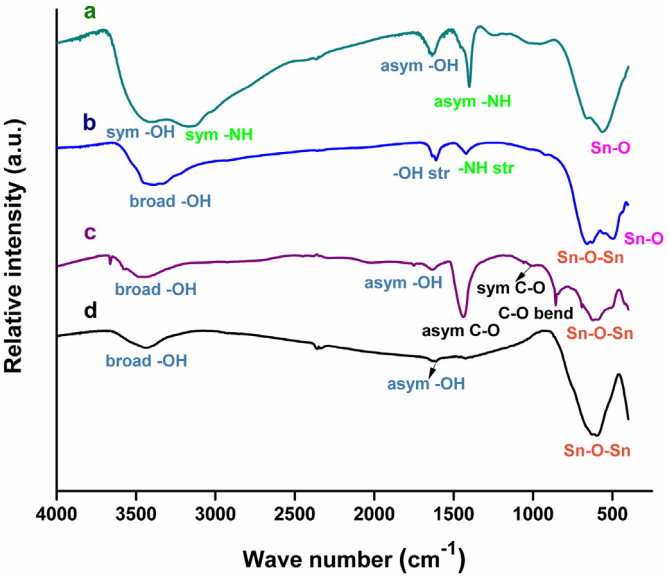

Fig. 3. A comparative FTIR study of a) $Sn(OH)_4$ b) B2SO (Ba/Sn 1:2) c) 2BSO (Ba/Sn 2:1) and d) BSO (Ba/Sn 1:1).

In case of B2SO, stoichiometrically excess Sn remained in form of SnO_2 which was stipulated by corresponding Sn–O peak at 528 cm^{-1} in Fig. 3b.

3.1.4. X-ray photoelectron spectroscopic (XPS) analysis

Elemental composition and the oxidation state of the constituents of BSO catalyst were evaluated by XPS analysis. The intrinsic peaks in the wide XPS spectra of BSO (Fig. 4A) suggested the presence of constituent elements as Ba, Sn and O. The oxidation state of the individual elements was confirmed by analyzing their core level spectrum. Fig. 4B has showed the 3d spectrum of barium (Ba) which indicates two sharp peaks at the binding energy (B.E.) of 778.7 eV and 794 eV. These binding energies correspond to the spin orbit doublet $Ba3d_{5/2}$ and $Ba3d_{3/2}$ respectively. The definite difference of 15.3 eV between these two peaks has confirmed that +2 oxidation state of Ba. Fig. 4C, the 3d spectrum of tin (Sn) yields two peaks correspond to the spin orbit doublet $Sn3d_{5/2}$ and $Sn3d_{3/2}$ at the B.E. of 486 eV and 494.4 eV respectively. The peak difference of 8.4 eV between two spin states has good agreements with the presence of Sn^{4+} in BSO. The deconvoluted 1s spectra of oxygen (Fig. 4D) has implied presence of two type of oxygen species in BSO. The lower B.E. of 530 eV corresponds to the fully coordinated oxygen of metal oxide; whereas, comparatively higher B.E. of 532 eV has assigned for hydroxide species which arise due to moisture contamination (John et al., 2019). Hence, it has invariably concluded that BSO existed as $BaSnO_3$ constituted with Ba^{2+}, Sn^{4+} and O^{2-}.

3.1.5. Scanning electron microscope (SEM) with energy dispersive X-ray (EDAX) analysis

The surface topology of the synthesized catalysts was viewed by scanning electron microscope (SEM). Pure SnO_2, synthesized by precipitation method as described in 2.2 was characterized by SEM to visualize its surface texture. In Fig. 5A it has clearly viewed that SnO_2 particles were smaller in size and existed in agglomerated form. The SEM image of uncalcined BSO in Fig. 5B comprises fully agglomerated mixed phases of $Sn(OH)_4$ and $Ba(NO)_3$ (Xie and Zhao,

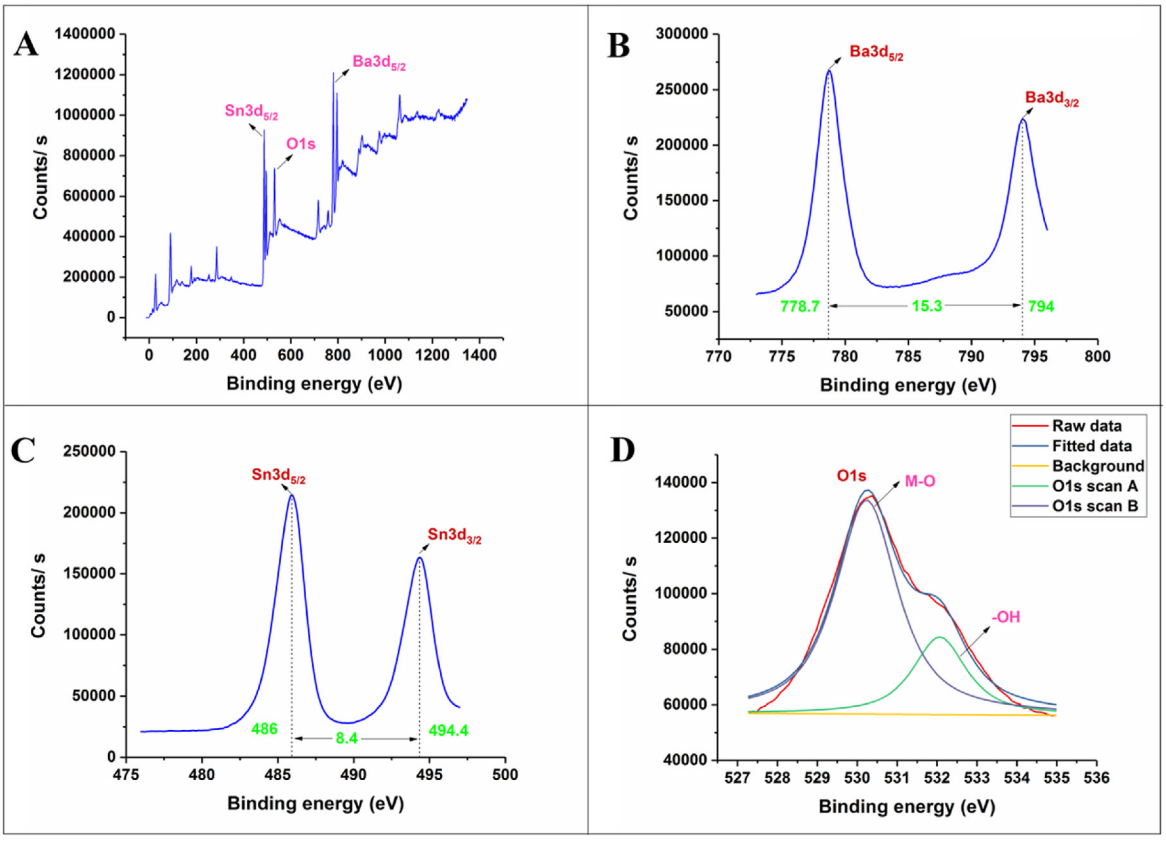

Fig. 4. XPS of BSO catalyst; A) wide spectra, B) 3d spectrum of Ba, C) 3d spectrum of Sn, D) 1s spectrum of O.

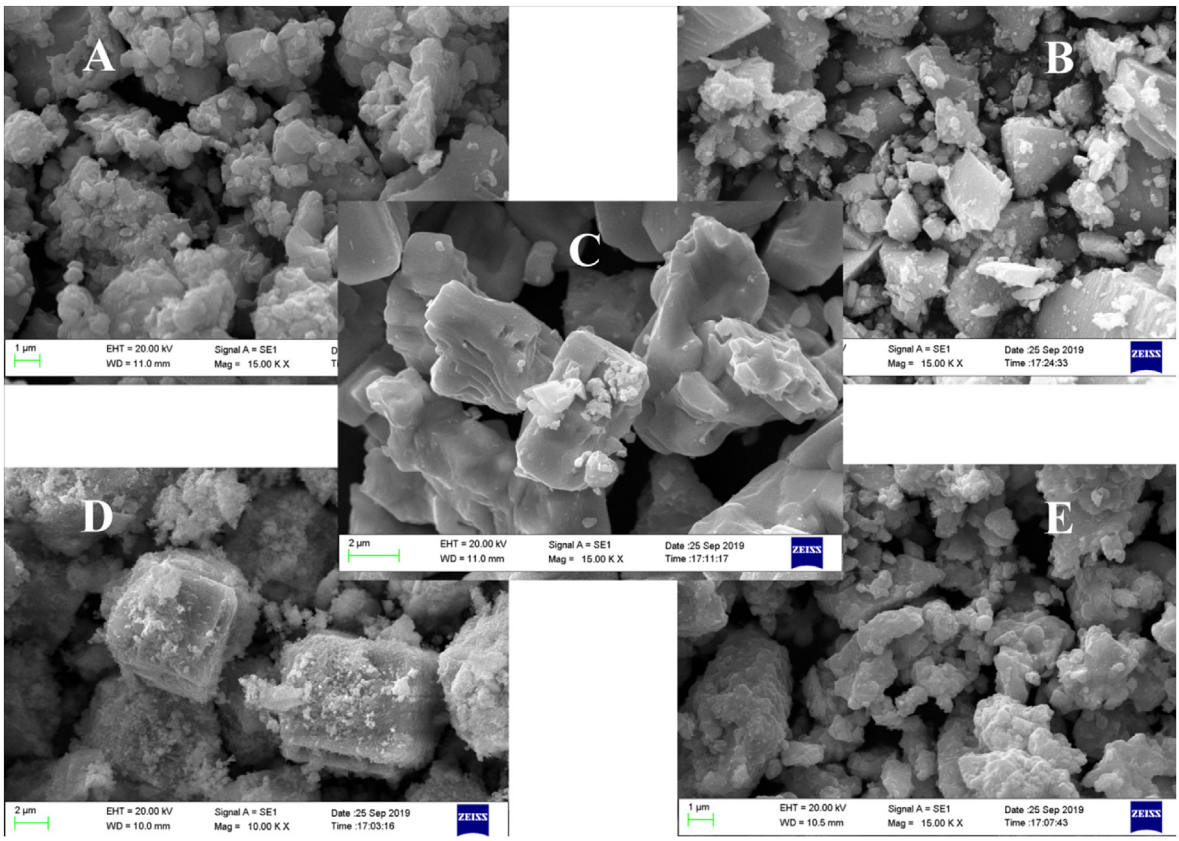

Fig. 5. SEM image of A) SnO_2 B) uncalcined BSO (Ba/Sn 1:1) C) calcined BSO (Ba/Sn 1:1) D) 2BSO (Ba/Sn 2:1) E) B2SO (Ba/Sn 1:2).

2013). After calcination at 850 °C, BSO showed smooth texture of catalytic surface as shown Fig. 5C. The particles of $BaSnO_3$ are seemed quite large and irregular in shape compare to pure SnO_2. In case of 2BSO (Ba/Sn 2 : 1) the SEM image (Fig. 5D) displays scattered deposition of $BaCO_3$ over $BaSnO_3$. When the stoichiometric ratio of Sn was increased to 1 : 2, the excess tin formed its native oxide which introduced more heterogeneity in particle shape, size and texture. Fig. 5E, the SEM of B2SO (Ba/Sn 1 : 2) implies that excess SnO_2 has randomly accommodated over the catalytic surface. The Ba/Sn atomic ratio of barium stannate catalyst samples was cross-verified by Energy-dispersive X-ray spectroscopy. The EDX spectra of perovskite $BaSnO_3$ having 1 : 1 Ba/Sn atomic ratio is attached in supplementary information file as Fig. S1. The atomic % and weight % of constituent atoms (Ba, Sn, O) present in barium stannate samples were included in the Table S1 (see supplementary information).

3.1.6. Brunauer-emmett-teller (BET) surface area analysis and basicity analysis

Both surface area and basic strength of a catalyst have synergistic impact on transesterification reaction. Table 2 comprises all the surface information as surface area, pore volume, pore size of the barium stannate samples having different Ba/Sn atomic ratio. It was obtained that BET surface area of pure perovskite $BaSnO_3$ catalyst (Ba/Sn 1:1) was larger than that of other barium stannate samples as 2BSO, B2SO. It was also noticed that pore size distribution of the catalyst BSO was found in mesoporous range of 2–50 nm (Sahani et al., 2019) which is very much appreciated for base catalyzed transesterification reaction. The reason behind the issue of lowering surface area of 2BSO and B2SO may be the scattered distribution of the native oxides and carbonates of stoichiometrically excess components over the active surface of $BaSnO_3$. This all justifications regarding BET analysis of the barium stannate samples have been deliberated by the mean of SEM information. Next, the most important catalytic property i.e. basicity of catalyst samples (SnO_2, BSO, 2BSO and B2SO) were rationalised by Hammett indicator benzene carboxylic acid titration method (as describe in section 2.3). The total basicity of the catalysts were calculated by adding the individual basicity at three different pK_a range, derived by using different indicators as mentioned in section 2.3. Pure SnO_2 shows nil basic strength, whereas, BSO, 2BSO and B2SO catalysts have basic strength of 1.44, 0.87, 0.64 mmol/g respectively in the range of 8.2 (phenolphthalein indicator) ‹ H_› 15.4 (2,4-dinitro-aniline). Such result clearly implies that pure SnO_2 had no basic site to interact with reactants but barium stannate samples had the appreciable basicity to act as an efficient

Table 2
Surface analysis of barium stannate compounds by BET adsorption-desorption.

Sample	Surface area (m^2/g)	Pore volume (cm^2/g)	Pore diameter (nm)
BSO (Ba:Sn 1 : 1)	144.09	0.5578	28.34
2BSO (Ba:Sn 2 : 1)	26.88	0.0115	67.54
B2SO (Ba:Sn 1 : 2)	5.83	0.0069	58.03

heterogeneous catalyst in transesterification reaction. In comparison, BSO had the highest basic strength, whereas excessive presence of carbonate species in 2BSO and SnO_2 in B2SO lowered the basic strength to greater extent. This happened due to acidic nature of both carbonate and SnO_2 (Xie et al., 2011). Moreover, it is anticipated that the basic Ba−O bond in $BaSnO_3$ may play as an active site for probable interaction with triglyceride molecule.

3.2. Gas chromatography (GC) of feedstock oils

The constituent fatty acid componants of the feedstock was ascertained by GC analysis. The gas chromatogram of waste cooking oil has been attached as Fig. 6. The mass spectra of individual componants having specific retaintion time in GC were identified using NIST database. The major fatty acid componants of WCO were palmitic acid (13.09%), stearic acid (5.04%), oleic acid (30.53%), linoleic acid (45.86%), α-linolenic acid (3.56%) having retention time 8.61, 11.47, 11.71, 12.25, 12.85 min respectively in GC. The minor componants were lauric acid, myristic acid, myristoleic, palmitoleic acid, arachidic acid, paullinic acid, behenic acid possessed total contribution of 2%. It has been also assorted that the feedstock contented by both unsaturated and saturated fatty acids as shown in Table S2 (see supplementry information).

3.3. Optimization of influencing factors in transesterification

The entire optimization process was designed by the means of various parameters under the consideration of their significant contribution in FAME conversion. The following important variables as Ba/Sn atomic ratio, catalyst activation temperature, oil to methanol molar ratio, catalyst weight %, reaction temperature, and time were optimized to achieve the maximum conversion of triglyceride to FAME. To investigate the individual impact of these factors on FAME conversion a series of transesterification reactions were conducted over a precise range taking one variable at a time (OVAT). Furthermore, the derived biodiesel was estimated by ^1H NMR to evaluate the percentage of FAME conversion ascribed in section 2.4. The outcomes of such optimization studies are discussed elaborately in the following subheads with the respective graphs.

3.3.1. Optimization of Ba/Sn atomic ratio and catalyst calcination temperature

For immense catalytic efficacy of $BaSnO_3$ in transesterification, it is very necessary to optimize the Ba/Sn atomic ratio and catalyst calcination temperature. Thus, to verify the optimum stoichiometric ratio in $BaSnO_3$ both metal concentrations were varied. Fig. 7A displays that among all barium stannate samples Ba/Sn atomic ratio 1 : 1 has obtained as the best stoichiometric ratio. This may occurred due to synergistic effect of large surface area and higher basicity. In case of 2BSO having 2 : 1 Ba/Sn atomic ratio showed lower catalytic activity due to lower surface area and lower basic strength as compare to BSO. However, B2SO (Ba/Sn 1 : 2) catalyst showed meager FAME conversion as the excess and catalytically inactive SnO_2 was randomly accumulated over $BaSnO_3$ and block the active sites. Thus it caused poor accessibility of the triglyceride molecule at the active sites (Sahani et al., 2019). Aftermath, the optimum calcination temperature of the catalyst BSO was explored by conducting a set of batch reactions using BSO catalyst calcined at different temperature varying from 550 to 950 °C at following reaction condition as oil to methanol molar ratio 1 : 16, catalyst dose 2.5 wt%, reaction temperature 65 °C for 25 min time duration. Fig. 7B has displayed that fatty acid methyl ester conversion was accelerated with elevating calcination temperature from 550 to 850 °C but slightly decreased at 950 °C. Maximum FAME conversion of 98% was obtained at 850 °C which has been considered as optimum value. This observation has been corroborated by the information getting from TGA and XRD analysis of the catalyst BSO. Increment in catalyst activation temperature up to 850 °C endorsed pure $BaSnO_3$ perovskite phase which was supposed to be the active phase in methyl esterification of WCO (Sahani and Sharma, 2018). On the other hand, reduction in FAME conversion at a calcination temperature beyond 850 °C was occurred may be due to significant deformation in active site at high temperature. Finally, the catalyst having optimized Ba/Sn atomic ratio 1 : 1 and optimized catalyst activation temperature 850 °C was introduced in other optimization studies as discussed below.

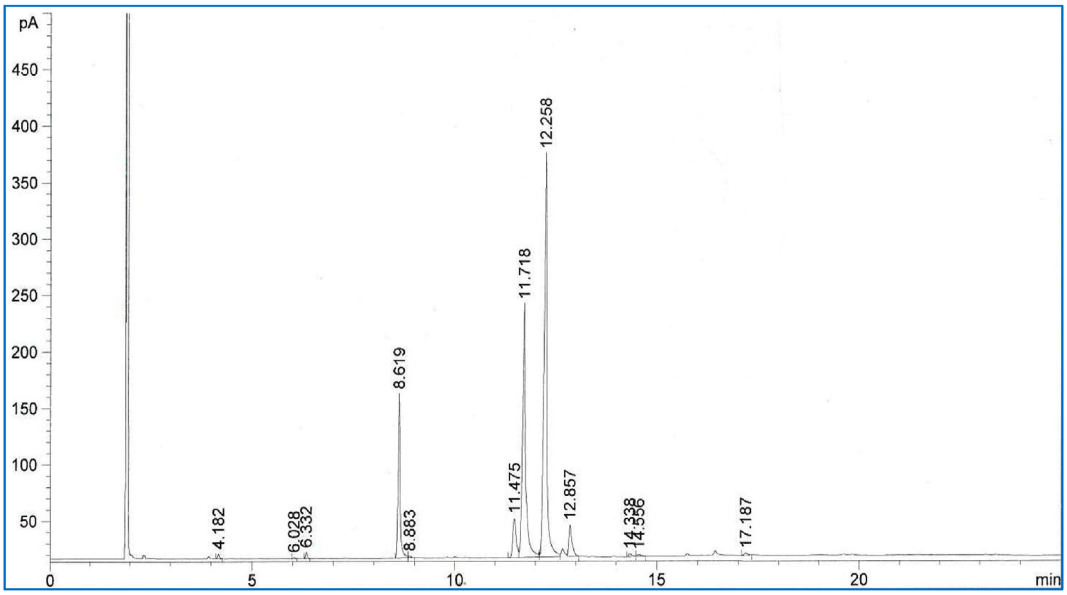

Fig. 6. Gas chromatogram of waste cooking oil.

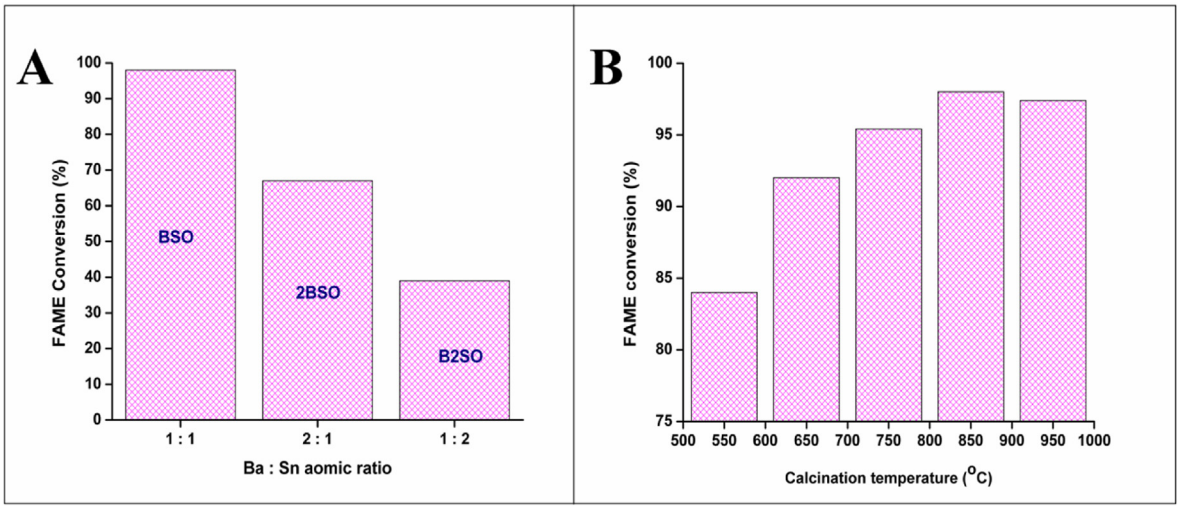

Fig. 7. Optimization of A) Ba/Sn stoichiometric ratio B) calcination temperature in FAME conversion from waste cooking oil.

3.3.2. Optimization oil to methanol molar ratio and catalyst weight percentage

According the literature, heterogeneous FAME conversion demands relatively more time and higher molar concentration of alcohol for prominent mass transfer between different phases as solid catalyst, polar methanol and non polar triglyceride (Xie and Huang, 2006). Basically, in transesterification reaction, all surface reactions are reversible (as shown in equations (3a), (3b) and (3c)); in consequence, to get the maximum methyl ester conversion, the reactions should be executed in presence of excess methanol to shift the equilibria towards forward direction for completion the reaction (Leclercq et al., 2001). So, the optimization of oil to methanol molar ratio is very much required. The influence of oil to methanol molar ratio on FAME conversion (%) was investigated by varying the molar ratio from 1:4 to 1:24 under the following reaction condition: catalyst weight 2.5 wt%, temperature 65 ± 0.5 °C, time 25 min. Fig. S 2A (see supplementary information) reveals that the highest FAME conversion was obtained at oil to methanol molar ratio 1: 16. Initially, FAME conversion was enhanced with increasing oil to methanol molar ratio, but after getting the optimum molar ratio it started to decrease with further increment in molar ratio. This whole phenomenon can be elaborated by lightning on the previous studies and hypothesis. At initial, incrimination in methanol concentration probably stimulated the mass transfer between three phases oil-methanol-catalyst (Putra et al., 2018). But at higher molar concentration of methanol, there were two possibilities for reducing FAME conversion. One was the shifting of reaction equilibrium toward the reactant side which might stimulated the backward reaction and second was the partial dissolution of glycerol in overabundant methanol which intern complicated the product phase separation and deduced the FAME conversion (Dai et al., 2015). Next, the effect of catalyst weight % in transesterification was investigated by varying catalyst amount from 0.5 to 3 wt% (w/w) with 0.5 wt% increment. The impact of catalyst weight % on methyl esterification has been shown in Fig. S 2B (see supplementary information), which has depicted that methanolysis is highly influenced by the amount of catalyst as it accounts the number of actual active sites exposed over the catalyst surface. More catalyst provides more accessibility of the reactants to accommodate and carry out the desire reaction. Thus transesterification was accelerated with increasing catalyst amount to the extent of the optimum value, i.e. 2.5 wt %. However, larger amount than that of optimum catalyst weight percentage increased the viscosity in reaction medium which consequently decreased the mass transfer between the heterogeneous phases (catalyst-oil-methanol). Thus it showed slightly low conversion after the optimum catalyst weight %. This similar phenomenon has also been observed by Sahani et al. (2018) and Roy et al. (2019).

3.3.3. Optimization of reaction temperature and time

In transesterification reaction, temperature is one of key parameters which require to be optimized to acquire the desire conversion percentage of product. An optimum temperature provides the require energy to overcome the threshold energy barrier. The optimized temperature was acquired by conducting a set transesterification reactions over a temperature range of 35 ± 0.5 to 75 ± 0.5 °C. The influence of temperature on FAME conversion of WCO using BSO catalyst has represented in Fig. S 2C (see supplementary information) which has implied that FAME conversion was accelerated when temperature was enhanced from ambient to optimum extent but at higher temperature above the optimum temperature it fell down instantly. Here, the optimum temperature of the WCO transesterification using BSO catalyst was found at 65 ± 0.5 °C near the boiling temperature of methanol. Many reports regarding on kinetics of transesterification have stated that this type of reactions are passing through endothermic pathway (Roy et al., 2019). In addition, the Lee Chateleir's principle states that the reaction equilibrium of an endothermic reaction will be shifted more towards the product side by enhancing reaction temperature. Thus it may be considered that such transesterification of WCO using BSO catalyst also follows the endothermic pathway (further investigated in kinetics part). At optimum temperature, the desire reaction acquires its threshold energy for completion the transesterification reaction. But when the reaction was performed at high temperature above the boiling temperature of methanol (64.7 °C), a significant amount of methanol evaporated which could not take part in the reaction and consequently FAME conversion fell down (Ayoub et al., 2017; Singh et al., 2016a,b). Last but not the least, optimization of reaction time is also very important for economic biodiesel production. Fig. S 2D (see supplementary information) presents FAME conversion of WCO using BSO catalyst at different time interval. For heterogeneous catalysis, the rate of the mass transfer invariably depends on effective contact period between interactive phases. Due to poor miscibility of three phases as solid catalyst, polar methanol and non polar triglyceride, heterogeneous transesterification takes comparatively more time than

others (Singh et al., 2019). Thus it is very obvious that FAME conversion will definitely be promoted with extending the reaction period due to better mass transfer. The maximum of 98% FAME conversion was achieved within 25 min at other optimum reaction condition. Beyond the optimum extent the reaction got the equilibrium as shown in Fig. S 2D (see supplementary information).

3.4. ^{1}H NMR analysis of oil and derived biodiesel

Fig. 8A and 8B correspond to the ^{1}H NMR spectra of WCO and its derived biodiesel. The NMR signals of WCO (shown in **Fig. 8**A) has been assigned as: chemical shift δ (ppm) = 5.41to 5.34 and 5.33 to 5.27 (m, -CH=CH-), 4.33 to 4.30 and 4.18 to 4.14 (d-d, CH−O and CH_2−O), 2.80 to 2.77 (t, C=C−CH_2−C=C), 2.34 to 2.31 (t, -OCO-CH_2), 2.07 to 2.04 (m, CH_2−C=C), 1.63 (s, CH_2−C−C=O), 1.32 to 0.98 (m, CH_2), 0.88 (m, CH_3). ^{1}H NMR spectra of derived biodiesel is alike of its feedstock along with unique differences which ultimately assure the biodiesel formation. The characteristic signals regarding triglyceride backbone (−CH_2-O and −CH-O) at chemical shift value 4.3 to 4.2 ppm present in ^{1}H NMR spectra of WCO (**Fig. 8**A) become disappear but the confirmatory signal for methyl esterification of triglyceride has been noticed at 3.7 ppm corresponds to methoxide proton (-OC**H**$_3$) as shown in Fig. 8B (Ba et al., 2016). This particular information rely that fatty acid methyl ester or biodiesel has formed as the product of transesterification of WCO.

3.5. Physico-chemical and fuel properties of derived biodiesel

Some important physico-chemical and fuel properties of derived FAME were ascertained by American Society for Testing

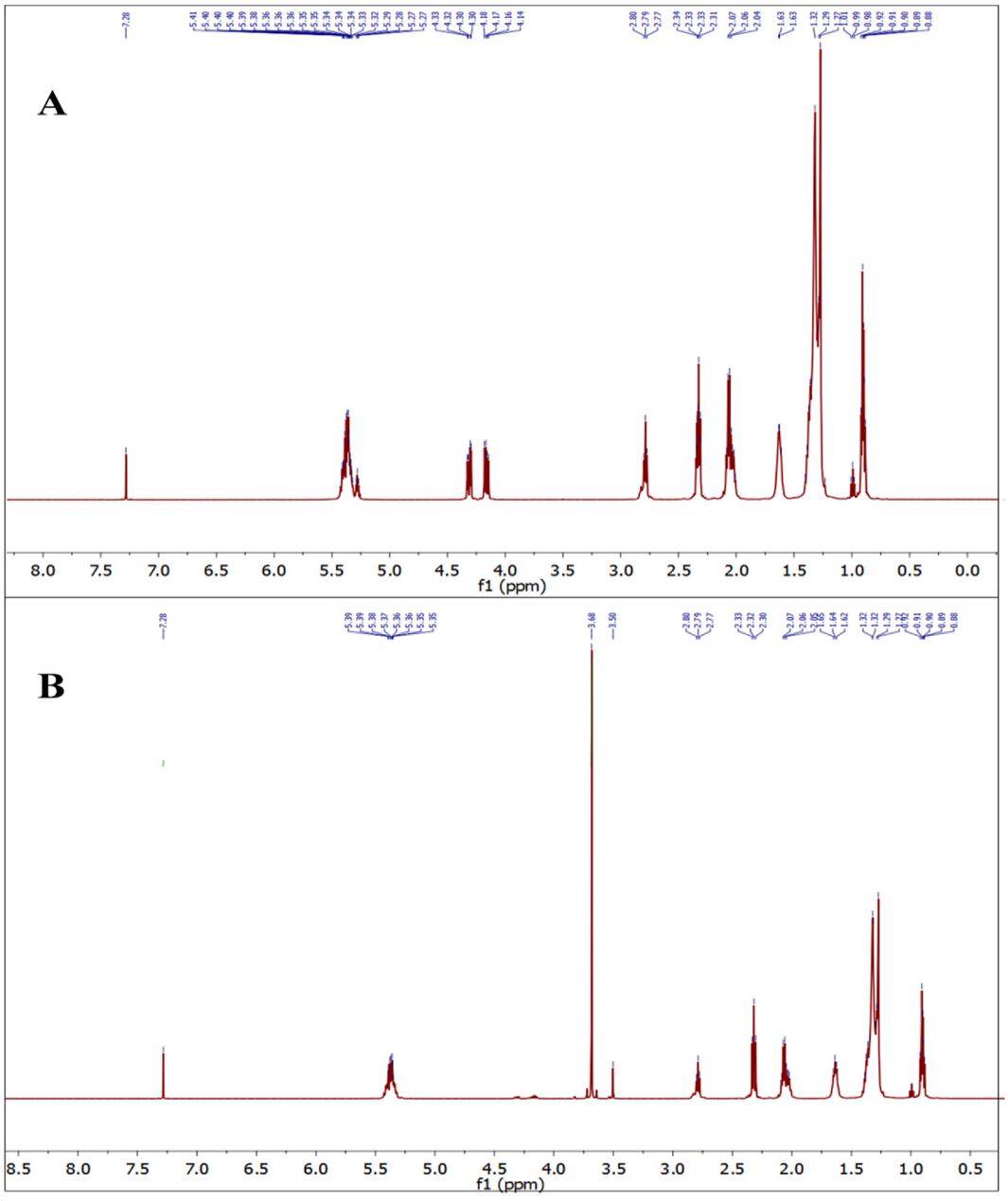

Fig. 8. ^{1}H NMR of A) waste cooking oil and B) synthesized biodiesel.

Table 3
Fuel properties of synthesized biodiesel.

Parameters	ASTM test method used	ASTM-6751 biodiesel	Biodiesel derived from WCO
Color	Nil	Nil	colorless
Acid value (mgKOH/g)	D 664	˂0.8	0.5
Kinematic viscosity (mm^2/s)	D 7110	1.9 to 6.0	4.3
Density (40 °C,$g.l^{-1}$)	D 4052	0.86–0.90	0.89
Calorific value (MJ/Kg)	D 240	35	41.34
Cetane number	D 613	47	49
Flash point (°C)	D 93	100 to 170	140
Cloud point (°C)	D2500	−3 to 12	2
Pour point (°C)	D 97-05	−15 to 16	6

and Materials (ASTM). The feasibility of synthesized biodiesel as a substitute of petrodiesel was decided with respect to various fuel properties as per ASTM D6751 standards (Roy et al., 2019). Table 3 represents the important properties as color, acid value, kinematic viscosity, density, calorific value, cetane number, flash point, cloud point, and pour point of the biodiesel derived from WCO. All such aforementioned properties were obtained within the acceptable limit for biodiesel as per ASTM standard. So, it assures that the produced biodiesel has immense potential to be an alternative fuel of petrodiesel.

3.6. Assessment of kinetic and thermodynamic parameters

The kinetic and thermodynamic parameters as rate constant, activation energy, pre-exponential factor, enthalpy of activation, entropy of activation and Gibb's free energy of activation for transesterification process using BSO catalyst were investigate by definite equations as described in section 2.5. Three sets of transesterification reactions were employed at three different temperatures (45, 55 & 65 °C) under the following reaction condition: 1:16 oil to methanol molar ratio, 2.5 wt% catalyst weight, time 25 min. After each 5 min interval the FAME conversions were estimated to derive the value of X_{FAME} in equation (8) (see section 2.5). $-\ln(1-X_{FAME})$ Vs time (min) was plotted for three distinct temperature to determine the respective rate constants by the mean of their corresponding slope of the above linear fits. In Fig. 9A, the respective kinetic plot at different reaction temperatures clearly demonstrate that rate of the reaction only depends upon triglyceride concentration. This can be stated as the regression values (0.96–0.98) has suggested good agreement with the anticipating pseudo first order kinetic modeling for biodiesel production from waste cooking oil using BSO catalyst (discussed in section 2.5). The derived rate constants were obtained to be 0.113 min^{-1} at 65 °C, 0.055 min^{-1} at 55 °C and 0.026 min^{-1} at 45 °C. It has seemed that rate constant will be increased 2–3 fold by increasing reaction temperature 10–20 °C. Next, the activation energy was determined by the help of Arrhenius plot (Fig. 9B) as derived in equation (10) (see section 2.5). The activation energy (E_a) and the frequency factor (A) were calculated to be 61.57 kJ/mol and 3.6×10^8 min^{-1} respectively. The activation energy endures in range of the base catalyzed heterogeneous reaction which is 33.6–84 kJ/mol (Lee et al., 2014). Aftermath, the thermodynamic parameters were evaluated from the Eyring-Polanyi plot ln(k/T) Vs ln(1/T) as shown in Fig. 9C. Enthalpy of activation ($\Delta H^{\#}$), entropy of activation ($\Delta S^{\#}$), and Gibb's free energy of activation ($\Delta G^{\#}$) of the reaction were obtained to be 59.76 kJ/mol, - 87.19 J/mol/K and 89.23 kJ/mol respectively. Both $\Delta H^{\#}$ and $\Delta G^{\#}$ had positive sign, which intimated that the reaction followed the non spontaneous endothermic pathway. Moreover, the negative sign of $\Delta S^{\#}$ implies that reduction in randomness occurred during the reaction.

3.7. Eley-Rideal (E-R) mechanism

A plausible mechanism of transesterification of WCO using BSO catalyst has been proposed on the basis of theoretical assumptions of previous studies. Primarily it was evaluated that pure SnO_2 had no catalytic efficiency to convert triglyceride to FAME but significant incorporation of barium showed impressive activity. So, it can be invariably stated that the basic nature of the Ba–O bond in $BaSnO_3$ is only responsible for its catalytic behavior in transesterification process. By this concept and the information regarding FTIR study of fresh catalyst and 5th time reused catalyst (washed and recalcined) displayed in Fig. S3 (see supplementary information) the plausible mode of interactions between reactants and catalyst have been shown in Fig. 10. In this FTIR study, the used catalyst was not washed thoroughly by methanol. After complete reaction, it was isolated from reaction mixture, then washed only one time with 5 ml methanol and left to dry under sun burn. According to Fig. 10, in step I, triglyceride was adsorbed to the active site and interacted with Ba–O bond. However, many researchers imply that first mode of interaction would takes place between basic bond and methanol which subsequently produced methoxide ion as the active species (Yadav and Sharma, 2019). But in our case no characteristic peak regarding OMe bond was found in FTIR spectra of washed catalyst (Fig. S 3b, see supplementary information)). So, conventional pathway (L-H mechanism) was not followed in case of transesterification using BSO catalyst. Moreover, pH of both WCO and methanol was tested and it was found that pH of WCO (5.8) was lower than that of methanol (6.7). Thus, a primary idea was developed that in initial interaction of triglyceride and catalyst may occur. Further, the characteristic IR frequencies in Fig. S 3b corresponds to double bonded C–H signal at 3006 cm^{-1}, single bonded C–H signal at 2923 cm^{-1} & 2854 cm^{-1}, carbonyl C–O signal at 1741 cm^{-1}, C=C signal at 1648 cm^{-1}, -C-O-C signal at 1161 cm^{-1}, and CH_2 wagging at 964 cm^{-1} confirming the feasibility the above assumption (adsorption of triglyceride on to catalyst) as revealed in step I of proposed E-R mechanism. Step II is involved in methanolysis reaction with adsorbed triglyceride and methanol. The mode interaction was designed by following basic concept of nucleophilic reaction. Step III has revealed that formation of by-product glycerol by insertion of hydrogen atom to the adsorbed glycerin backbone. It was also proved by FTIR spectra of washed catalyst. Due to irreversibility some of the glycerol molecule was still adsorbed at the active site. The characteristic broad peak at around 3436 cm^{-1} assigned for –OH stretching in (**Fig S 3b, see supplementary information)** has assured about the presence of glycerol on the catalyst surface. Considering all the justifications regarding interaction modes confirmed by FTIR analysis, it is stated that the transesterification of WCO using BSO catalyst followed the E-R mechanism rather than conventional L-H mechanism.

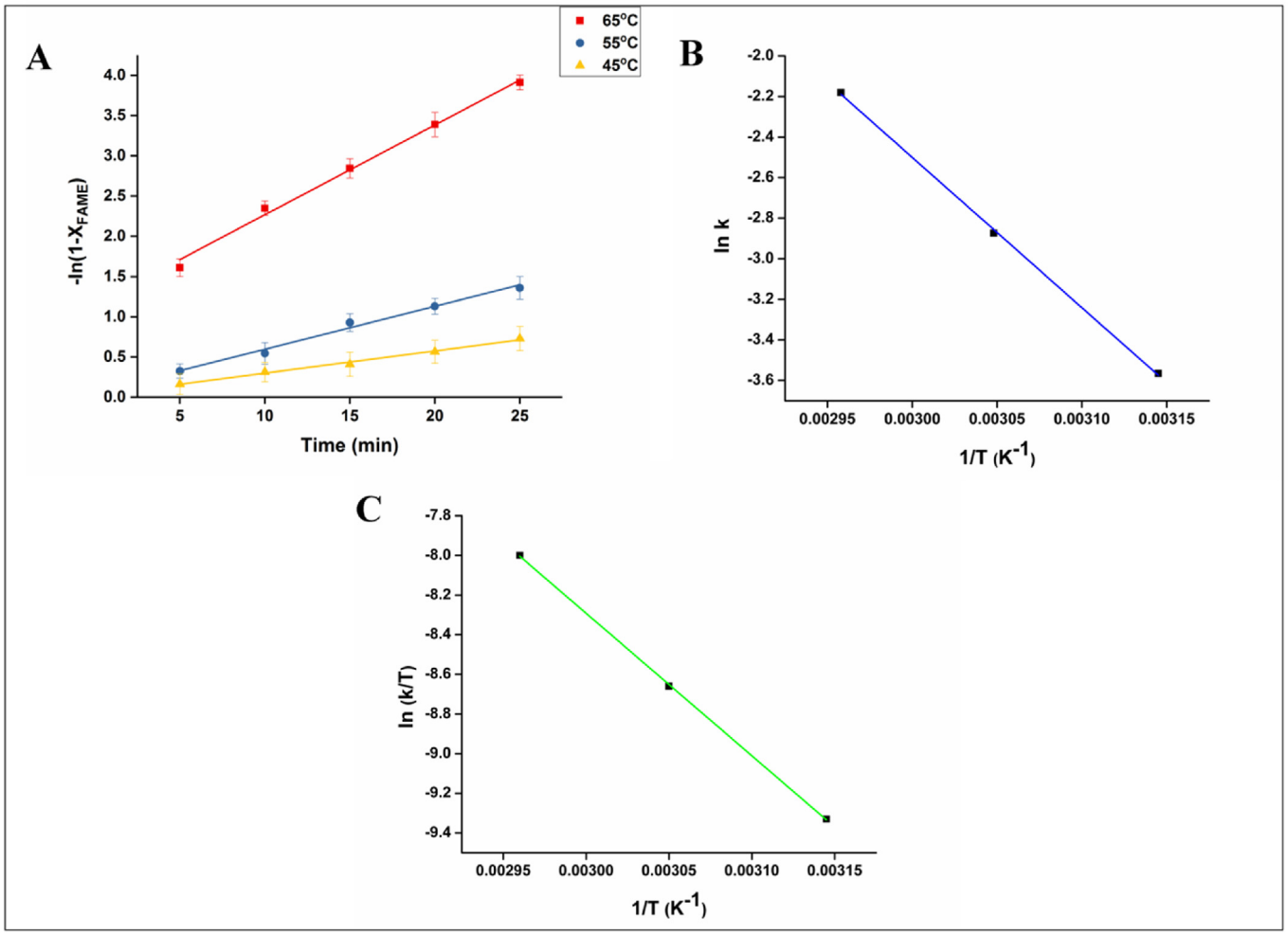

Fig. 9. A) Kinetic plot $-\ln(1-X_{FAME})$ Vs Time in min B) Arrhenius plot lnk Vs 1/T in K^{-1} C) Eyring – Polanyi plot ln(k/T) Vs 1/T in K^{-1}

3.8. Catalyst endurance test

One of the important reasons to choose heterogeneous catalyst over homogeneous catalyst for transesterification is its recyclability or endurance capacity. To investigate the endurance capacity of catalyst BSO in transesterification of WCO required reactivation of the catalytic ability after each catalytic run. Such reactivation was acquired by the following process: **Step 1-** after completion the reaction, the BSO catalyst was recovered from the mixture by easy filtration method then washed with methanol and ethanol subsequently. **Step 2-** the washed catalyst was put into an air dry oven for 8 h. **Step 3-** the dried catalyst was recalcined at 600 °C for 2 h to decompose the residual organic species (triglyceride and glycerol) which were still stuck to the pores after washing. But complete regeneration of the catalyst was not accompanied because of high affinity of barium towards carbonates derived from decomposition of residual organic matter in recalcination process. The comparative FTIR spectra (Fig. S3, see supplementary information) of fresh catalyst, washed catalyst and recalcined catalyst confirms the facts regarding catalytic poisoning through pore clogging by organic groups (different C–H stretching, CH_2 stretching & carbonyl CO stretching) and presence of abundant carbonate species (1459, 1370 & 856 cm^{-1} of carbonate C–O stretching). Thus basicity of the catalyst was affected due to acidic nature of sustained carbonate species. The FAME conversion at each catalyst cycle has been shown in Fig. S4 (see supplementary information) and it was found that FAME conversion was decreased to 81.6% after 5th run of BSO catalyst. This above phenomenon has explained on basis of basicity of the used catalyst which effectively influenced the FAME conversion. The basic strength or basicity of the used catalyst samples have been shown in Table S3 (see supplementary information) which has informed that basicity was simultaneously decreased from 1st to 5th run. It might happen due to increase the amount of carbonate species at the active site after each cycle. Herewith, considering the endurance potency and the conversion capacity, it is definitely stated that the catalyst BSO is an efficient catalyst for economic production of biodiesel from waste cooking oil. A comparative study of such BSO catalyst with the previously reported catalysts also suggests that it is superior among all (Table 4).

3.9. Study on turnover frequency and 'greenness' of the catalytic cycles

The potency of the catalyst has been judged with regards to turnover frequency (TOF) defining the number of moles of product formed per basic site per time (sec) (Abdul et al., 2015) as shown in **equation (15)**. Table S3 (see supplementary information) has enlisted the turnover frequencies of the catalyst in five consecutive run. The BSO catalyst has high TOF which almost comparable with the homogeneous catalyst i.e. H_2SO_4 (Sani et al., 2014). The catalytic efficiency of the catalyst was retained up to 3rd cycle but at 4th and 5th cycle it was going to decrease. This may be happened due to

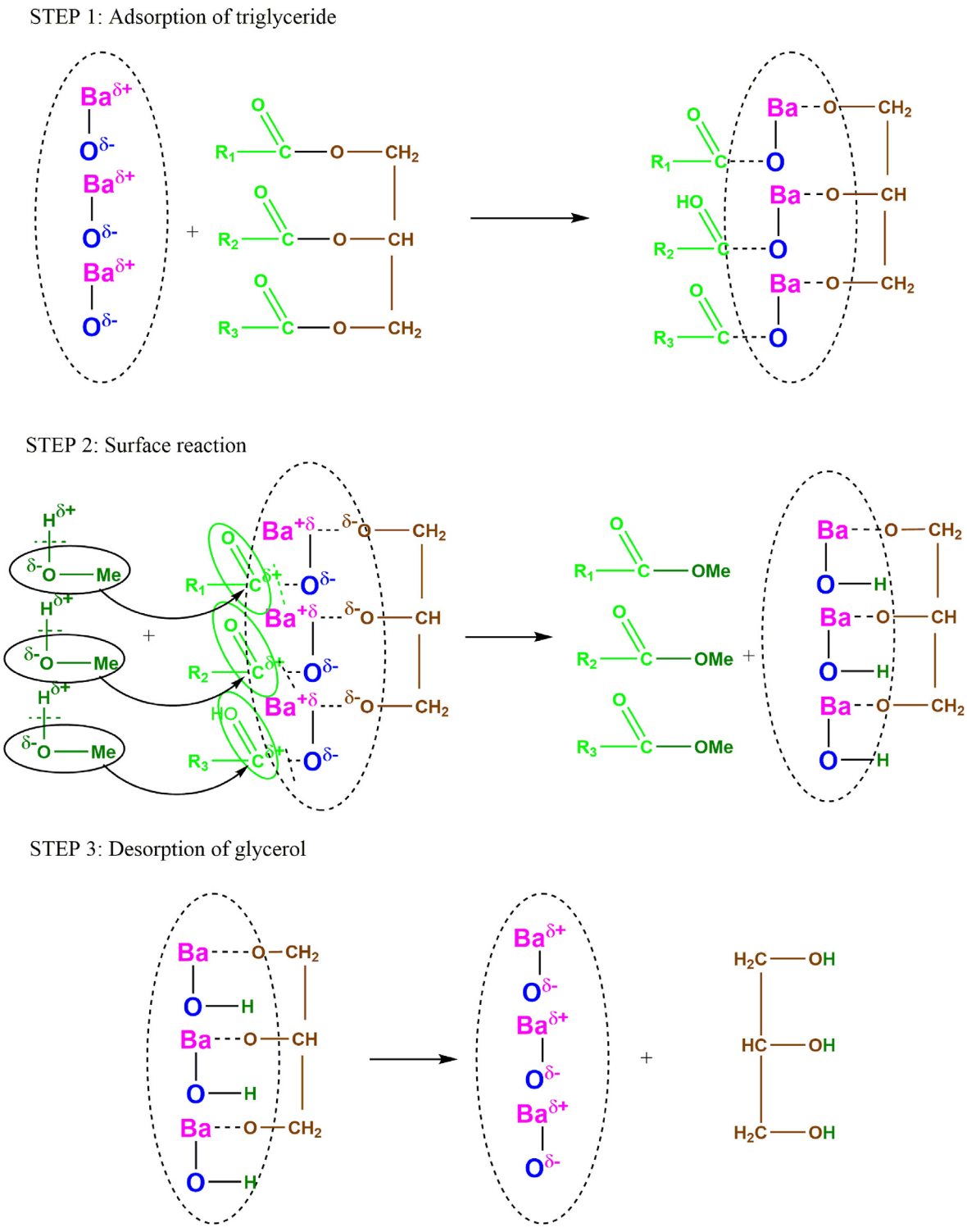

Fig. 10. Mechanism of base catalyzed transesterification of WCO using BSO catalyst.

poor basic strength led the reduction in biodiesel production after 3rd catalytic run.

$$\text{Turnover frequency or TOF} = \frac{moles\ of\ product\ or\ biodiesel\ (mol)}{basicity\ (mmol) \times time\ (\text{sec})} \quad (15)$$

According to the postulates of green chemistry one of the important points is "lower waste generation during any chemical reaction is considered as greener process." This means a clean process should produce lower amount of waste. Thus the waste production during catalytic cycles was necessarily investigated to confirm how much the process would be green. So, the extent of 'greenness' of transesterification process using BSO catalyst was analyzed under consideration of two important parameters as Environment factor and Process Mass Index. Environmental factor

Table 4
A comparative study of catalytic activity of barium based heterogeneous catalysts in biodiesel production.

Catalyst name	Feedstock	Method	Conversion (C) or Yield (Y)	Comment	Reference
BaO	Soybean oil	Transesterification	Y = 95%	Required very high temperature(215 °C)	Singh and Fernando (2007)
BaO	Refined rapeseed oil	Transesterification	C = 86%	Required high catalyst dose of 10 wt% and longer reaction time of 3.5h	Yan et al. (2007)
BaO	Palm oil	Ultrasonic-assisted transesterification (50% amplitude)	Y = 95.2%	Cost ineffective process	Mootabadi et al. (2010)
KOH/La−Ba −Al_2O_3	Microalgae oil	Transesterification	C ≥ 95%	Catalyst deactivation occurs when KOH incorporated more than 30%	Zhang et al. (2012)
Ba/CaO	Waste cooking oil	Transesterification	C = 88%	Comparatively poor conversion	Balakrishnan et al. (2013)
$BaZrO_3$	P. pinnata oil	Transesterification	C = 98±0.5%	3h long reaction duration	Singh et al. (2016) a,b
Barium lanthanum oxide	Madhuca oil	Transesterification	C = 97.5%	Catalyst deactivation due to passivation of organic moiety	Sahani and Sharma (2018)
Cs modified $BaZrO_3$	Millettia Pinnata oil	Transesterification	C = 97.27%	Very long duration of 23h	Kumar and Singh (2019)
$BaCeO_3$	Karanja oil	Transesterification	C = 98.41%	Taking comparative longer time of 100 min	Sahani et al. (2019)
$BaSnO_3$	**Waste cooking oil**	**Transesterification**	**C = 98%**	**Excellent efficiency with long durability, high TOF and clean process**	**This work**

is illustrated as weight of waste produced per weight of product or biodiesel (in gram); whereas, PMI defines the total mass used in the process per gram of biodiesel production (Yadav and Sharma, 2019).

$$\text{E} - \text{factor} = \frac{\textit{weight of waste } (g)}{\textit{weight of the product } (g)} \quad (16)$$

$$\text{PMI} = \frac{\textit{weight of mass used in process } (g)}{\textit{weight of product } (g)} \quad (17)$$

Waste production till 5th catalyst run has been shown in Fig. 11A. Glycerol as byproduct of FAME was considered as a waste which was definitely formed in each cycle. Initially up to 3rd cycle only glycerol was founded as waste. So that, the E-factors for 1st to 3rd cycle were observed to be very low (as shown in Table S3, see supplementary information); which actually implies that the process is absolutely non-hazardous to the environment. After 3rd cycle E-factor was increased due to addition of waste methanol which was previously distilled and reused. The highest E-factor was obtained at 5th cycle as discarded catalyst weight was added along with waste methanol and glycerol.

It was noticed (in Table S3, see supplementary information) that basicity, the key factor of the catalytic activity was decreased after each cycle. As an obvious result, reduction in biodiesel production from 1st to 5th cycle was obtained. Consequently, the PMI was increased from 1st to 5th cycle, which means economic productivity of biodiesel should be hampered after each catalytic run. So, an overview has developed that the catalyst BSO is very much efficient to catalyze transesterification of waste cooking oil up to three consecutive run without causing any severe environmental issue. The overall waste generation during complete life of catalyst BSO (five consecutive run) has been shown as pie chart of Fig. 11B. It is clearly viewed that the methanol and glycerol have the major contribution in waste generation of biodiesel production. But in these, glycerol can be further used to synthesis various value-added products like glycerol carbonate, ɣ-lactic acid etc. So, advanced

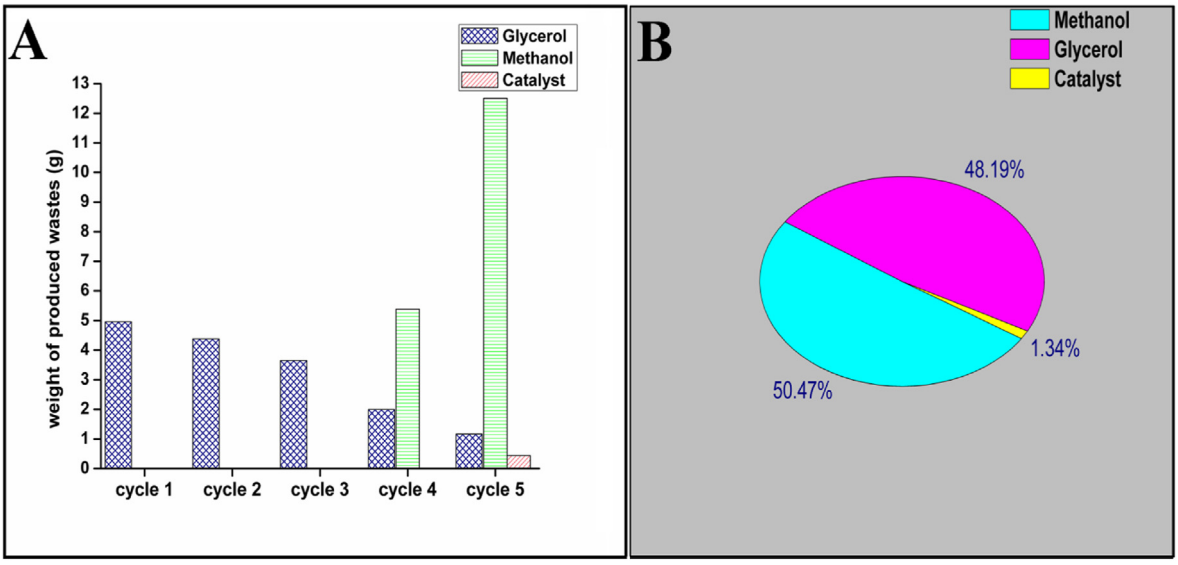

Fig. 11. A) Production of waste per catalytic run; B) Pie chart of overall waste production in entire catalytic life of five cycles.

processing of glycerol should favor the waste management in biodiesel production.

4. Conclusion

Barium stannate compounds with 1:1, 1:2 and 2:1 Ba:Sn stoichiometric ratio were synthesized via wet impregnation method. Then various physical properties as thermal stability, phase formation, presence of functional group, surface topology, BET surface area and basic strength of the prepared catalysts were investigated through various techniques. Among these three stoichiometrically different barium stannate compound, $BaSnO_3$ or BSO (Ba:Sn 1:1) activated at 850 °C showed best catalytic performance in transesterification of WCO. The qualitative and quantitative analysis of synthesized biodiesel was carried out by proton NMR. The maximum conversion was obtained to be 98% at the following optimum reaction condition: as 1 : 16 oil to methanol molar ratio, 2.5 wt% catalyst weight, 65 °C temperature and 25 min time. Then some important physico-chemical properties of the synthesized biodiesel as acid value, calorific value, cetane number, viscosity, density, flash point, etc were checked and found within the permissible limit prescribed by ASTM D6751 standard. This means that product biodiesel would be a good substitute of petrodiesel in using C.I engine.

Well fitted kinetic plot suggested that reaction followed pseudo-first order kinetics; moreover, corresponding signs of thermodynamic parameters implied that reaction went on endothermic non-spontaneous pathway. On the basis of FTIR result of used catalyst E-R mechanism has been designed for transesterification of WCO using BSO catalyst. The assessment of recyclability reveals that the BSO is a sustainable catalyst for biodiesel production for showing commendable activity of 81.6% up to 5th catalytic run. Moreover, TOF and E-metrics of the complete life of the BSO catalyst were examined which proposed that the catalyst has remarkable efficiency and contribute to cleaner production of biodiesel up to three catalytic run. So, overall it is concluded that biodiesel production from WCO using BSO catalyst is an economic and greener approach.

Declaration of competing interest

The authors declare that they have no known competing financial interests or personal relationships that could have appeared to influence the work reported in this paper.

CRediT authorship contribution statement

Tania Roy: Data curation, Formal analysis, Methodology, Validation, Writing - original draft. **Shalini Sahani:** Data curation, Formal analysis, Methodology, Validation, Writing - original draft. **Devarapaga Madhu:** Data curation, Formal analysis. **Yogesh Chandra Sharma:** Conceptualization, Project administration, Methodology, Funding acquisition, Writing - review & editing.

Appendix A. Supplementary data

Supplementary data related to this article can be found at https://doi.org/10.1016/j.jclepro.2020.121440.

References

Abdul, R.Y., Abdu, M.B., Aminuddin, R., Kamaluddeen, S.K., 2015. Catalytic performance by kinetics evaluation of novel KOH-modified zinc oxide in the heterogeneous transesterification of rice bran oil to biodiesel. Int. Proc. Chem. Bio. Environ. Eng. 84, 101–107.

Ayoub, M., Bhat, A.H., Ullah, S., Ahmad, M., Uemura, Y., 2017. Optimization of biodiesel production over alkaline modified clay catalyst. J. Jpn. Inst. Energy 96 (10), 456–462.

Ba, S., Zhang, H., Lee, Y.J., Ng, C.W., Li, T., 2016. Chemical modifications of ricinolein in castor oil and methyl ricinoleate for viscosity reduction to facilitate their use as biodiesels. Eur. J. Lipid Sci. Technol. 118 (4), 651–657.

Balakrishnan, K., Olutoye, M.A., Hameed, B.H., 2013. Synthesis of methyl esters from waste cooking oil using construction waste material as solid base catalyst. Bioresour. Technol. 128, 788–791.

Birla, A., Singh, B., Upadhyay, S.N., Sharma, Y.C., 2012. Kinetics studies of synthesis of biodiesel from waste frying oil using a heterogeneous catalyst derived from snail shell. Bioresour. Technol. 106, 95–100.

Bošković, I.V., Vukčević, M., Nenadović, S.S., Mirković, M.M., Stojmenović, M., Pavlović, V.B., Kljajević, L.M., 2019. Characterization of red mud/metakaolin-based geopolymers as modified by $Ca(OH)_2$. Mater. Technol. 53 (3), 341–348.

Bozbas, K., 2008. Biodiesel as an alternative motor fuel: production and policies in the European Union. Renew. Sustain. Energy Rev. 12 (2), 542–552.

Chen, C., Cai, L., Zhang, L., Fu, W., Hong, Y., Gao, X., Jiang, Y., Li, L., Yan, X., Wu, G., 2020. Transesterification of rice bran oil to biodiesel using mesoporous NaBeta zeolite-supported molybdenum catalyst: experimental and kinetic studies. Chem. Eng. J. 382, 122839.

Conti, J., Holtberg, P., Diefenderfer, J., LaRose, A., Turnure, J.T., Westfall, L., 2016. International Energy Outlook 2016 with Projections to 2040. Washington, DC (United States).

Dai, Y.M., Wu, J.S., Chen, C.C., Chen, K.T., 2015. Evaluating the optimum operating parameters on transesterification reaction for biodiesel production over a $LiAlO_2$ catalyst. Chem. Eng. J. 280, 370–376.

Deepa, A.S., Vidya, S., Manu, P.C., Solomon, S., John, A., Thomas, J.K., 2011. Structural and optical characterization of $BaSnO_3$ nanopowder synthesized through a novel combustion technique. J. Alloys Compd. 509 (5), 1830–1835.

Encinar, J., Pardal, A., Sánchez, N., Nogales, S., 2018. Biodiesel by transesterification of rapeseed oil using ultrasound: a kinetic study of base-catalysed reactions. Energies 11 (9), 2229.

Galvan, D., Orives, J.R., Coppo, R.L., Silva, E.T., Angilelli, K.G., Borsato, D., 2013. Determination of the kinetics and thermodynamics parameters of biodiesel oxidation reaction obtained from an optimized mixture of vegetable oil and animal fat. Energy Fuel. 27 (11), 6866–6871.

Hardy, J.T., 2003. Climate Change: Causes, Effects, and Solutions. John Wiley & Sons.

Hashimoto, K., Masuda, T., Motoyama, H., Yakushiji, H., Ono, M., 1986. Method for measuring acid strength distribution on solid acid catalysts by use of chemisorption isotherms of Hammett indicators. Ind. Eng. Chem. Prod. Res. Dev. 25 (2), 243–250.

John, J., Chalana, S.R., Prabhu, R., Pillai, V.M., 2019. Effect of oxygen pressure on the structural and optical properties of $BaSnO_3$ films prepared by pulsed laser deposition method. Appl. Phys. A 125 (3), 155.

Kljajević, L.M., Melichova, Z., Kisić, D.D., Nenadović, M.T., Todorović, B.Ž., Pavlović, V.B., Nenadović, S.S., 2019. The influence of alumino-silicate matrix composition on surface hydrophobic properties. Sci. Sinter. 51 (2), 163–173.

Knothe, G., 2010. Biodiesel and renewable diesel: a comparison. Prog. Energy Combust. Sci. 36 (3), 364–373.

Kumar, D., Singh, B., 2019. $BaZrO_3$ and Cs-$BaZrO_3$ catalysed transesterification of Millettia Pinnata oil and optimisation of reaction variables by response surface Box-Behnken design. Renew. Energy 133, 411–421.

Kwon, S., Lee, S.G., Chung, E., Lee, W.R., 2015. CO_2 adsorption on H_2O-saturated BaO (1 0 0) and induced barium surface dissociation. Bull. Kor. Chem. Soc. 36 (1), 11–16.

Lam, M.K., Lee, K.T., Mohamed, A.R., 2009. Sulfated tin oxide as solid super acid catalyst for transesterification of waste cooking oil: an optimization study. Appl. Catal. B Environ. 93 (1–2), 134–139.

Leclercq, E., Finiels, A., Moreau, C., 2001. Transesterification of rapeseed oil in the presence of basic zeolites and related solid catalysts. J. Am. Oil Chem. Soc. 78 (11), 1161–1165.

Lee, A.F., Bennett, J.A., Manayil, J.C., Wilson, K., 2014. Heterogeneous catalysis for sustainable biodiesel production via esterification and transesterification. Chem. Soc. Rev. 43 (22), 7887–7916.

Martinez-Guerra, E., Gude, V.G., 2014. Transesterification of used vegetable oil catalyzed by barium oxide under simultaneous microwave and ultrasound irradiations. Energy Convers. Manag. 88, 633–640.

Mierczynski, P., Ciesielski, R., Kedziora, A., Maniukiewicz, W., Shtyka, O., Kubicki, J., Albinska, J., Maniecki, T.P., 2015. Biodiesel production on MgO, CaO, SrO and BaO oxides supported on $(SrO)(Al_2O_3)$ mixed oxide. Catal. Lett. 145 (5), 1196–1205.

Mladenović, N., Kljajević, L., Nenadović, S., Ivanović, M., Čalija, B., Gulicovski, J., Trivunac, K., 2020. The applications of new inorganic polymer for adsorption cadmium from waste water. J. Inorg. Organomet. Polym. 30 (2), 554–563.

Mohadesi, M., Hojabri, Z., Moradi, G., 2014. Biodiesel production using alkali earth metal oxides catalysts synthesized by sol-gel method. Biofuel Res. J. 1 (1), 30–33.

Mootabadi, H., Salamatinia, B., Bhatia, S., Abdullah, A.Z., 2010. Ultrasonic-assisted biodiesel production process from palm oil using alkaline earth metal oxides as the heterogeneous catalysts. Fuel 89 (8), 1818–1825.

Mucsi, G., 2017. Physical-chemical, mineralogical and radiological properties of red mud samples as secondary raw materials. Nucl. Technol. Radiat. Protect. 1452–8185. ISSN 1451-3994, ESSN.

Nenadović, S.S., Kljajević, L.M., Nešić, M.A., Petković, M.Ž., Trivunac, K.V., Pavlović, V.B., 2017. Structure analysis of geopolymers synthesized from clay originated from Serbia. Environ. Earth Sci 76 (2), 79.

Omer, A.M., 2008. Energy, environment and sustainable development. Renew. Sustain. Energy Rev. 12 (9), 2265–2300.
Patil, P.D., Deng, S., 2009. Transesterification of camelina sativa oil using heterogeneous metal oxide catalysts. Energy Fuel. 23 (9), 4619–4624.
Putra, M.D., Irawan, C., Ristianingsih, Y., Nata, I.F., 2018. A cleaner process for biodiesel production from waste cooking oil using waste materials as a heterogeneous catalyst and its kinetic study. J. Clean. Prod. 195, 1249–1258.
Roy, A., Das, P.P., Selvaraj, P., Sundaram, S., Devi, P.S., 2018. Perforated $BaSnO_3$ nanorods exhibiting enhanced efficiency in dye sensitized solar cells. Sustain. Chem. Eng. 6 (3), 3299–3310.
Roy, T., Sahani, S., Sharma, Y.C., 2019. Study on kinetics-thermodynamics and environmental parameter of biodiesel production from waste cooking oil and castor oil using potassium modified ceria oxide catalyst. J. Clean. Prod. 119166.
Sahani, S., Sharma, Y.C., 2018. Economically viable production of biodiesel using a novel heterogeneous catalyst: kinetic and thermodynamic investigations. Energy Convers. Manag. 171, 969–983.
Sahani, S., Banerjee, S., Sharma, Y.C., 2018. Study of co-solvent effect on production of biodiesel from Schleichera Oleosa oil using a mixed metal oxide as a potential catalyst. J. Taiwan Inst. Chem. Eng. 86, 42–56.
Sahani, S., Roy, T., Sharma, Y.C., 2019. Clean and efficient production of biodiesel using barium cerate as a heterogeneous catalyst for the biodiesel production; kinetics and thermodynamic study. J. Clean. Prod. 237, 117699.
Sakthiraj, K., Hema, M., Kumar, K.B., 2018. The effect of reaction temperature on the room temperature ferromagnetic property of sol-gel derived tin oxide nanocrystal. Phys. B Condens. Matter 538, 109–115.
Sani, Y.M., Daud, W.M.A.W., Aziz, A.A., 2014. Activity of solid acid catalysts for biodiesel production: a critical review. Appl. Catal. Gen. 470, 140–161.
Singh, A.K., Fernando, S.D., 2007. Reaction kinetics of soybean oil transesterification using heterogeneous metal oxide catalysts. Chem. Eng. Technol.: Ind. Chem. Plant Equip. Process Eng. Biotechnol. 30 (12), 1716–1720.
Singh, V., Bux, F., Sharma, Y.C., 2016a. A low cost one pot synthesis of biodiesel from waste frying oil (WFO) using a novel material, β-potassium dizirconate (β-$K_2Zr_2O_5$). Appl. Energy 172, 23–33.
Singh, V., Hameed, B.H., Sharma, Y.C., 2016b. Economically viable production of biodiesel from a rural feedstock from eastern India, P. pinnata oil using a recyclable laboratory synthesized heterogeneous catalyst. Energy Convers. Manag. 122, 52–62.
Singh, R., Kumar, A., Sharma, Y.C., 2019. Biodiesel production from microalgal oil using barium–calcium–zinc mixed oxide base catalyst: optimization and kinetic studies. Energy Fuel. 33 (2), 1175–1184.
Su, M., Yang, R., Li, M., 2013. Biodiesel production from hempseed oil using alkaline earth metal oxides supporting copper oxide as bi-functional catalysts for transesterification and selective hydrogenation. Fuel 103, 398–407.
Wu, X., Lv, G., Hu, X., Tang, Y., 2012. A two-step method to synthesize $BaSn(OH)_6$ crystalline nanorods and their thermal decomposition to barium stannate. J. Nanomater. 2012.
Xie, W., Huang, X., 2006. Synthesis of biodiesel from soybean oil using heterogeneous KF/ZnO catalyst. Catal. Lett. 107 (1–2), 53–59.
Xie, W., Zhao, L., 2013. Production of biodiesel by transesterification of soybean oil using calcium supported tin oxides as heterogeneous catalysts. Energy Convers. Manag. 76 (2013), 55–62.
Xie, W., Wang, H., Li, H., 2011. Silica-supported tin oxides as heterogeneous acid catalysts for transesterification of soybean oil with methanol. Ind. Eng. Chem. Res. 51 (1), 225–231.
Yadav, M., Sharma, Y.C., 2019. Transesterification of used vegetable oil using $BaAl_2O_4$ spinel as heterogeneous base catalyst. Energy Convers. Manag. 198, 111795.
Yan, S., Lu, H., Liang, B., 2007. Supported CaO catalysts used in the transesterification of rapeseed oil for the purpose of biodiesel production. Energy Fuel. 22 (1), 646–651.
Yang, R., Su, M., Li, M., Zhang, J., Hao, X., Zhang, H., 2010. One-pot process combining transesterification and selective hydrogenation for biodiesel production from starting material of high degree of unsaturation. Bioresour. Technol. 101 (15), 5903–5909.
Zhang, X., Ma, Q., Cheng, B., Wang, J., Li, J., Nie, F., 2012. Research on KOH/La-Ba-Al_2O_3 catalysts for biodiesel production via transesterification from microalgae oil. J. Nat. Gas Chem. 21 (6), 774–779.